Biogeosciences Discuss., doi:10.5194/bg-2016-222, 2016
Manuscript under review for journal Biogeosciences
Published: 3 June 2016

Biogeosciences Discussions Open Access EGU

A manuscript submitted to discussion forum of BG as a BG discussion paper (bg-2016-222):

Manganese and iron reduction dominate organic carbon oxidation in deep continental margin sediments of the Ulleung Basin, East Sea

Jung-Ho Hyun[1]*, Sung-Han Kim[1], Jin-Sook Mok[1], Hyeyoun Cho[1], Tongsup Lee[2], Verona Vandieken[3] and Bo Thamdrup[4*]

[1]Department of Marine Sciences and Convergent Technology, Hanyang University, 55 Hanyangdaehak-ro, Ansan, Gyeonggi-do 15588, South Korea

[2]Department of Oceanography, Pusan National University, Busan 609-735, South Korea

[3]Institute for Chemistry and Biology of the Marine Environment, University of Oldenburg, Carl-von-Ossietzky-Str. 9-11, 26129 Oldenburg, Germany

[4]Nordic Center for Earth Evolution, Department of Biology, University of Southern Denmark, Campusvej 55, 5230 Odense M, Denmark

*Correspondence to:
Jung-Ho Hyun (hyunjh@hanyang.ac.kr)
Bo Thamdrup (bot@biology.sdu.dk)

Biogeosciences Discuss., doi:10.5194/bg-2016-222, 2016
Manuscript under review for journal Biogeosciences
Published: 3 June 2016

Abstract. Rates and pathways of benthic organic carbon (C_{org}) oxidation were investigated in surface sediments of the Ulleung Basin (UB) characterized by high organic carbon contents (> 2.5 %, dry wt.) and very high concentrations of Mn oxides (> 200 μmol cm^{-3}) and Fe oxides (up to 100 μmol cm^{-3}). The combination of geochemical analyses and independently executed metabolic rate measurements revealed that Mn and Fe reduction were the dominant C_{org} oxidation pathways in the center of the UB, comprising 45 % and 20 % of total C_{org} oxidation, respectively. By contrast, sulfate reduction was the dominant C_{org} oxidation pathway accounting for 50 % of total C_{org} mineralization in the continental slope. The relative significance of each C_{org} oxidation pathway matched the depth distribution of the respective electron acceptors. The relative importance of Mn reduction for C_{org} oxidation displays saturation kinetics with respect to Mn oxide content with a low half-saturation value of 8.6 μmol cm^{-3}, which further implies that Mn reduction can be a dominant C_{org} oxidation process even in sediments with lower MnO_2 content as known from several other locations. This is the first report of a high contribution of manganese reduction to C_{org} oxidation in offshore sediments on the Asian margin. The high manganese oxide content in the surface sediment in the central UB was maintained by an extreme degree of recycling, with each Mn atom on average being reoxidized ~3800 times before permanent burial. This is the highest degree of recycling so far reported for Mn-rich sediments, and it appears linked to the high benthic mineralization rates resulting from the high organic carbon content that indicate the UB as a biogoechemical hotspot for turnover of organic matter and nutrient regeneration. Thus, it is important to monitor any changes in the rates and partitioning of C_{org} oxidation to better understand the biogeochemical cycling of carbon, nutrients and metals associated with long-term climatic changes in the UB, where the fastest increase in sea water temperature has been reported for the past two decades.

Keywords. Benthic mineralization, Manganese reduction, Iron reduction, Sulfate reduction, Ulleung Basin, East Sea

Biogeosciences Discuss., doi:10.5194/bg-2016-222, 2016
Manuscript under review for journal Biogeosciences
Published: 3 June 2016

1 Introduction

Although they cover only 15 % (47 x 10^6 km^2) of the ocean surface area, sediments of continental margins (200 – 2000 m depth) are characterized by enhanced organic matter flux generated either by vertical transport from the highly productive overlying water column or by lateral transport from adjacent shelves, and thus play an important role in deposition and mineralization of organic matter (Romankevich, 1984, Jahnke et al., 1990; Walsh, 1991; Jahnke and Jahnke, 2000). Organic particles that reach the seafloor are quickly mineralized by hydrolysis, fermentation, and a variety of respiratory processes using different electron acceptors such as oxygen, nitrate, Mn oxides, Fe oxides, and sulfate (Froelich et al., 1979; Jørgensen, 2006). The partitioning of organic carbon (C_{org}) oxidation among the different electron accepting pathways has profound influence on the distribution and the release and/or retention of Mn, Fe, S and nutrients (nitrogen and phosphate) (Canfield et al., 2005; Jørgensen, 2006). Therefore, it is particularly important to elucidate the contribution of each C_{org} oxidation pathway in order to better understand the role of sediments in biogeochemical element cycles.

The relative significance of each carbon oxidation pathway is largely controlled by the combination of organic matter supply and availability of electron acceptors. In general, aerobic metabolism dominates the organic matter mineralization in deep-sea sediments that are characterized by low organic matter content (Jahnke et al., 1982; Glud, 2008). In contrast, owing to high sulfate concentrations in marine sediment, sulfate reduction accounts for up to 50 % of total carbon oxidation in continental margins with high organic matter flux (Jørgensen, 1982; Jørgensen and Kasten, 2006). However, in sediments where manganese and iron oxides are abundant or rapidly recycled, microbial reduction of manganese and iron can be the dominant electron accepting processes over sulfate reduction (Sørensen and Jørgensen, 1987; Aller, 1990; Canfield et al., 1993b). The significance of dissimilatory iron reduction for C_{org} oxidation is well established in the sediments of various continental margins and coastal wetlands (Thamdrup, 2000; Thamdrup and Canfield, 1996; Jensen et al. 2003, Kostka et al., 2002a, 2002b; Vandieken et al., 2006; Hyun et al., 2007, 2009b). However, only a few locations such as Panama Basin (Aller, 1990), the coastal Norwegian trough in Skagerrak and an adjacent fjord (Canfield et al., 1993a, 1993b; Vandieken et al., 2014), the Black Sea shelf (Thamdrup et al., 2000) and the continental shelf of the northern Barents Sea (Vandieken et al., 2006; Nickel et al., 2008) are known where microbial

Biogeosciences Discuss., doi:10.5194/bg-2016-222, 2016
Manuscript under review for journal Biogeosciences
Published: 3 June 2016

manganese reduction significantly contributes to carbon mineralization.

The East Sea (often referred to as Japan Sea), located in the far eastern part of the Eurasian continental margin, consists of three major basins deeper than 2,000 m, Japan Basin, Yamato Basin and Ulleung Basin (Fig. 1). Compared to the other two basins, the Ulleung Basin (UB) is characterized by higher phytoplankton biomass and primary production (Yamada et al., 2005; Yoo and Park, 2009), which is associated with coastal upwelling (Hyun et al., 2009a). The enhanced biological production in the water column is responsible for the high organic carbon content (> 2.5 % wt) in the sediment, and the highest rates of C_{org} oxidation compared to any other deep-sea sediments with similar depth range (Lee et al., 2008; Hyun et al., 2010). An intriguing geochemical property of the UB surface sediment is the high content of Mn oxides (> 200 μmol cm^{-3}) and Fe oxides (up to 100 μmol cm^{-3}) (Cha et al., 2007; Hyun et al., 2010). In accordance with these geochemical findings, the suppression of sulfate reduction (Hyun et al., 2010) and accumulation of Mn^{2+} in anoxic incubation of surface sediment (Vandieken et al., 2012) strongly implied that the C_{org} oxidation in the surface sediment of the UB is dominated by microbial manganese and iron reduction, but actual rates and partitioning of each electron accepting pathway in C_{org} oxidation remain to be determined in this deep marginal sediment underlying highly productive water column.

The primary objective of this paper was to characterize the sediment biogeochemistry with regard to the rate of C_{org} oxidation and partitioning of major terminal electron accepting pathways at two contrasting sites in the continental slope and rise in the UB. Here, for the first time in sediments of the Asian marginal seas, we document that Mn and Fe reduction are the dominant C_{org} oxidation pathways accounting for respectively 45 % and 20 % of total C_{org} oxidation in the center of the UB, and suggest that Mn and Fe reduction may be of greater importance in deep-sea sediments than previously recognized.

2 Materials and methods

2.1 Study site

Shipboard experiments were conducted in June, 2009 at two sites on the continental slope (M1) and rise (D3) in the center of the UB (Fig. 1, Table 1). Surface sediments consist of fine-grained clay with a mean grain size less than 0.004 mm in diameter (Cha et al., 2007).

Biogeosciences Discuss., doi:10.5194/bg-2016-222, 2016
Manuscript under review for journal Biogeosciences
Published: 3 June 2016

The two stations were characterized by the two contrasting sediment colors. The Mn oxide-enriched surface sediment at the basin site (D3) was reddish-brown, whereas at the slope site (M1) it exhibited the typical gray-brown color of muddy continental sediments (Fig. 1). Further environmental properties are listed in Table 1.

2.2 Sampling and handling

Sediment samples were collected with a box corer. Onboard, duplicate or mostly triplicate sub-samples for geochemical analyses were collected using acrylic cores (6–9 cm i.d.). The sub-cores for geochemical analyses were immediately sealed with butyl rubber stoppers and transferred to a N_2-filled glove bag for sectioning and loading into polypropylene centrifuge tubes that were then tightly capped and centrifuged for 15 min at 5000 × *g*. After reintroduction into the N_2-filled glove bag, pore-waters were sampled and filtered through 0.2-µm cellulose ester syringe filters (ADVANTEC, Toyo Rashi Kaisha, Ltd). One to two mL of pore water to determine NH_4^+ was fixed with saturated $HgCl_2$, and frozen. For determination of Fe^{2+}, Mn, SO_4^{2-} and Ca^{2+}, 2 mL of the pore water were acidified with 12M HCl and stored at 4 °C. Pore-water for sulfide analysis was preserved with Zn acetate (20 %). Sediments for solid-phase analysis were frozen at − 25 °C for future analyses.

2.3 Anoxic bag incubations

Anaerobic carbon mineralization rates and dissimilatory Mn and Fe reduction rates were determined in batch incubations based on the procedures of Canfield et al. (1993b) and Thamdrup and Canfield (1996). Sediment cores were transferred to a N_2-filled glove bag and sliced in 2-cm intervals to a depth of 10 cm. Sediment from parallel sections was pooled, mixed and loaded into gas-tight plastic bags (Hansen et al., 2000). The bags were sealed without gas space, and incubated in the dark at near in situ temperature (ca. 1 – 2 °C) in larger N_2 filled bags to ensure anoxic conditions. Over a period of 18 days of incubation, sub-samples to determine the accumulation of total dissolved inorganic carbon (DIC) and Mn in pore water were withdrawn on days 0, 1, 3, 5, 9 and 18. Two 50-mL centrifuge tubes per bag were filled completely with sediment in N_2-filled glove bag, and pore-water was extracted as described above. For DIC analysis, we collected 1.8 mL aliquots into glass vials without head space, fixed with 18 µL of $HgCl_2$ (125 mM), and stored at 4 °C until analysis in 4 weeks.

Biogeosciences Discuss., doi:10.5194/bg-2016-222, 2016
Manuscript under review for journal Biogeosciences
Published: 3 June 2016

Samples for Mn analysis were acidified with 12M HCl and stored at 4 °C. Sediment remaining after the collection of pore water was frozen at −25 °C for later analysis of oxalate extractable solid Fe(II).

2.4 Pore-water analyses

Total dissolved inorganic carbon (DIC) and NH_4^+ were measured by flow injection analysis with conductivity detection (Hall and Aller, 1992). Nitrate was measured spectrophotometrically (Parsons et al., 1984). Dissolved Fe^{2+} was determined by colorimetric method with Ferrozine (Stookey, 1970). Dissolved Mn and Ca^{2+} were analyzed in acidified pore water by inductive coupled plasma-atomic emission spectrometry (ICP-AES, Optima 3300DV, Perkin-Elmer Co.) and flame atomic absorption spectrometer (SpectrAA 220/FS, Varian), respectively (Thamdrup and Canfield, 1996). Dissolved sulfide was determined by the methylene blue method (Cline, 1969). Sulfate concentrations were measured using ion chromatography (Metrohm 761).

2.5 Solid-phase analyses

Total oxalate-extractable Fe [Fe(II) + Fe(III)] was extracted from air-dried sediment in a 0.2 M oxic oxalate solution (pH 3) for 4 h (Thamdrup and Canfield, 1996), and Fe(II) was extracted from frozen sediment in anoxic oxalate (Phillips and Lovley, 1987). The total oxalate-extractable Fe and Fe(II), hereafter total $Fe_{(oxal)}$ and $Fe(II)_{(oxal)}$, were determined as described in pore-water analysis of Fe^{2+}. Oxalate-extractable Fe(III), hereafter $Fe(III)_{(oxal)}$, was defined as the difference between total $Fe_{(oxal)}$ and $Fe(II)_{(oxal)}$. This fraction represents poorly crystalline Fe(III) oxides. Particulate Mn, hereafter $Mn_{(DCA)}$ was extracted with dithionite-citrate-acetic acid (DCA; pH 4.8) for 4 h from air-dried sediment and was determined by inductive coupled plasma-atomic emission spectrometry (ICP-AES, Optima 3300DV, Perkin-Elmer Co). The DCA extraction aims at dissolving free Mn oxides and authigenic Mn(II) phases. The reproducibility of the measurements was better than 10 % and the detection limits was 3 μM for Mn. For the determination of total reduced sulfur (TRS) that includes acid volatile sulfide (AVS = FeS + H_2S) and chromium-reducible sulfur (CRS = S^0 + FeS_2), sediment samples were fixed with Zn acetate, and sulfide was determined according to the method of Cline (1969) after a two-step distillation with cold 12 M HCl and

Biogeosciences Discuss., doi:10.5194/bg-2016-222, 2016
Manuscript under review for journal Biogeosciences
Published: 3 June 2016

198 boiling 0.5 M Cr^{2+} solution (Fossing and Jørgensen, 1989). The contents of particulate
199 organic carbon (POC) and nitrogen (PON) in the surface sediment were analyzed using a
200 CHN analyzer (CE Instrument, EA 1110) after removing $CaCO_3$ using 12 M HCl.
201
202 **2.6 Oxygen micro-profiles**
203
204 Oxygen profiles were measured at 50 µm resolution using Clark-type microelectrodes
205 (Unisense, OX-50) while stirring the overlying water. Microelectrodes were calibrated
206 between 100 % air-saturated *in situ* bottom water and N_2 purged anoxic bottom water. Three
207 profiles were measured at each site. The diffusive boundary layer (DBL) and sediment-water
208 interface (SWI) were determined according to Jørgensen and Revsbech (1985). To estimate
209 the volume-specific oxygen consumption rate, we used the PROFILE software (Berg et al.,
210 1998).
211
212 **2.7 Rate measurements**
213
214 The diffusive oxygen uptake (DOU) was calculated from the calibrated oxygen microprofiles.
215
216 $$DOU = - D_o \Delta C/\Delta z, \quad (1)$$
217
218 where D_o is the temperature-corrected molecular diffusion coefficient, and C is the oxygen
219 concentration at depth z within the diffusive boundary layer (DBL) (Jørgensen and Revsbech,
220 1985).
221 The volume-specific O_2 consumption rates exhibited a bimodal depth distribution with
222 activity peaks near the sediment-water interface and the oxic/anoxic interface, respectively.
223 Thus, O_2 consumption rates by aerobic organotrophic respiration was defined as the O_2
224 consumption rate near the sediment-water interface, whereas the oxygen consumption at the
225 oxic-anoxic interface was assigned to re-oxidation of reduced inorganic compounds
226 (Rasmussen and Jørgensen, 1992; Canfield et al., 2005).
227 Total anaerobic C_{org} mineralization rates were determined by linear regression of the
228 accumulation of total DIC with time during the anoxic bag incubations (Fig. 3) after
229 correcting for $CaCO_3$ precipitation (Thamdrup et al., 2000). Briefly, $CaCO_3$ precipitation was
230 calculated from decreasing soluble Ca^{2+} concentration during the anoxic bag incubation:

Biogeosciences Discuss., doi:10.5194/bg-2016-222, 2016
Manuscript under review for journal Biogeosciences
Published: 3 June 2016

$$\Delta CaCO_3 = \Delta[Ca^{2+}]_{sol} \times (1 + K_{Ca}), \quad (2)$$

where, K_{Ca} is the adsorption constant for Ca^{2+} (K_{Ca} = 1.6) (Li and Gregory, 1974). Then rate of DIC production rate corrected for $CaCO_3$ precipitation was calculated as:

$$\text{DIC production} = \text{DIC accumulation} + CaCO_3 \text{ precipitation} \quad (3)$$

Fe(III) reduction rates were determined by linear regression of the increase in solid-phase $Fe(II)_{(oxal)}$ concentration with time during anoxic bag incubations. The dissimilatory microbial Fe(III) reduction rate was derived by subtracting abiotic Fe reduction coupled to the oxidation of sulfide produced by sulfate reduction (Kostka et al., 2002b):

$$\text{Dissimilatory microbial Fe(III) Red} = \text{Total Fe(III) Red} - \text{Abiotic Fe(III) Red} \quad (4)$$

assuming that abiotic Fe reduction coupled to H_2S oxidation occurred at a stoichiometry of 2 Fe(III) per 3 H_2S (Pyzik and Sommer, 1981):

$$3H_2S + 2FeOOH = 2FeS + S^o + 4H_2O \quad (5)$$

Finally, to estimate the C_{org} oxidation by microbial Fe reduction, the 4:1 stoichiometry of iron reduction coupled to C_{org} oxidation was used from the stoichiometric equation (Canfield et al., 1993a):

$$CH_2O + 4FeOOH + 8H^+ = CO_2 + 4Fe^{2+} + 7H_2O \quad (6)$$

Mn reduction rates were determined from linear regression of the production of dissolved Mn^{2+} with time during the anoxic bag incubations. Similar to previous studies (e.g., Canfield et al., 1993a, 1993b; Thamdrup and Dalsgaard, 2000), we assumed that accumulating dissolved Mn was Mn^{2+}. This ignores a potential contribution from Mn^{3+}, which in some cases can constitute a substantial fraction of the dissolved Mn pool at the upper boundary of the zone with soluble Mn accumulation in marine sediments (Madison et al., 2013). Further studies of the dynamics of soluble Mn^{3+} are required to evaluate its potential importance in

Biogeosciences Discuss., doi:10.5194/bg-2016-222, 2016
Manuscript under review for journal Biogeosciences
Published: 3 June 2016

anoxic incubations. Such studies pending, we find justification for our assumption in the good agreement observed in the previous studies between Mn reduction rates calculated based on the assumption that soluble Mn is Mn^{2+} (Eq. 7) and independent estimates of rates of carbon mineralization through dissimilatory Mn reduction based on DIC or NH_4^+ accumulation. Due to strong adsorption of Mn^{2+} to Mn oxide surfaces, (Canfield et al., 1993b), the Mn reduction rates were estimated after compensating for the adsorption effect of Mn^{2+} to Mn-oxides according to Thamdrup and Dalsgaard (2000):

$$\text{Mn reduction rate} = Mn^{2+} \text{ accumulation rate} \times (1 + K^*_{Mn}{}^{2+} \times (1 - \Phi) \times \Phi^{-1} \times \delta_s) \quad (7)$$

where, Φ = porosity

δ_s = density of sediment

$K^*_{Mn}{}^{2+} = 4.8 + 0.14 \times [Mn(IV)]$ (ml g^{-1})

[Mn(IV)] = the concentration of Mn(IV) (μmol g^{-1})

We here assume that extracted $Mn_{(DCA)}$ represents Mn(IV) as observed in surface sediments of another Mn-rich site (Canfield et al., 1993b, Thamdrup and Dalsgaard, 2000). Small levels of $Mn_{(DCA)}$ remaining at depth further suggest that little Mn(II) accumulates in the solid phase (*see* Results). C_{org} oxidation by dissimilatory Mn(IV) reduction was calculated from the stoichiometric equation (Canfield et al., 1993a):

$$CH_2O + 2MnO_2 + 4H^+ = CO_2 + 2Mn^{2+} + 3H_2O \quad (8)$$

Sulfate reduction rates were determined using the radiotracer method of Jørgensen (1978). Sediment cores (35 cm long with 2.9 cm i.d.) were collected in triplicate, injected horizontally at 1-cm vertical interval with 5 μL radiolabeled sulfate ($^{35}S\text{-}SO_4^{2-}$, 15 kBq μl^{-1}, Amersham) diluted in sterilized NaCl solution (3.0 %), and incubated for 12 h at *in situ* temperature. At the end of the incubation, the sediment was sliced into sections, fixed in Zn acetate (20 %), and frozen at −25 °C until processed in the laboratory. The reduced ^{35}S was recovered using distillation with a boiling acidic Cr^{2+} solution according to Fossing and Jørgensen (1989). Background radioactivity of ^{35}S was 32.4±3.7 cpm cm^{-3} (n=10) at site D3 and 87.5±38.7 cpm cm^{-3} (n=10) at site M1. Detection limits of the SRR, estimated from the

Biogeosciences Discuss., doi:10.5194/bg-2016-222, 2016
Manuscript under review for journal Biogeosciences
Published: 3 June 2016

296 double standard deviation of the blank value (i.e., 7.4 and 77.4 cpm) according to Fossing et
297 al. (2000), ranged from 0.79 to 2.62 nmol cm^{-3} d^{-1}. To elucidate the contribution of sulfate
298 reduction in anaerobic carbon oxidation, the SRRs (Fig. 5B, 5G) were converted to carbon
299 oxidation using a stoichiometric equation (Thamdrup and Canfield, 1996):
300
301 $2CH_2O + SO_4^{2-} + 2H^+ = 2CO_2 + H_2S + 2H_2O$ (9)
302
303
304 **3 Results**
305
306 **3.1 Pore-water and solid-phase constituents**
307
308 The depth distributions of NH_4^+, NO_3^-, Mn^{2+} and Fe^{2+} in the pore-water as well as solid phase
309 Mn, Fe and S for the two stations are shown in Fig. 2. NH_4^+ concentrations at M1 increased
310 steadily with depth (Fig. 2A) whereas at D3 it decreased down to 3 cm depth before it
311 increased below (Fig. 2F). Highest concentrations of nitrate were measured at 0 to 1 cm
312 sediment depth at the two stations and concentrations decreased below a background level (<
313 2 µM) below 1 cm at both M1 and D3 (Fig. 2A, 2F). Dissolved Mn^{2+} concentrations differed
314 widely between the sites showing a maximum of 56 µM between 0 and 3 cm depth and not
315 exceeding 10 µM below at M1 (Fig. 2B), whereas at D3 concentrations increased to a
316 maximum of 286 µM at 10 – 12 cm depth (Fig. 2G). Conversely, dissolved Fe^{2+}
317 concentrations at M1 increased from 11 µM at 0 – 0.5 cm to 32 µM at 6 – 7 cm depth, and
318 stayed constant below (Fig. 2C), whereas at D3, concentrations were uniformly low showing
319 a slight increase to 12 µM at 15 cm (Fig. 2F).
320 Extractable Mn ($Mn_{(DCA)}$) concentrations were low (< 3 µmol cm^{-3}) in the upper 20 cm at
321 the slope site (M1) (Fig. 2B), but up to 200 µmol cm^{-3} in the upper 4 cm depth of the
322 sediment at the center of the basin (D3), with a sharp decrease to near depletion (~1 µmol
323 cm^{-3}) below 10 cm (Fig. 2G). At the slope site (M1), concentrations of $Fe(III)_{(oxal)}$ decreased
324 slightly with increasing depth from 28 µmol cm^{-3} near the surface to 13 µmol cm^{-3} at 20 cm
325 depth, mirroring an increase in $Fe(II)_{(oxal)}$ (Fig. 2D). At the center of the basin (D3),
326 $Fe(III)_{(oxal)}$ increased slightly from 67 µmol cm^{-3} at 0 – 0.5 cm to 90 µmol cm^{-3} at 4 – 6 cm
327 depth, and decreased steeply below to 4.8 µmol cm^{-3} at 12 – 14 cm depth (Fig. 2I). Of total

Biogeosciences Discuss., doi:10.5194/bg-2016-222, 2016
Manuscript under review for journal Biogeosciences
Published: 3 June 2016

328 $Fe_{(oxal)}$, $Fe(III)_{(oxal)}$ comprised > 98 % at 0 – 2 cm and > 97% at 0 – 8 cm depth at M1 and D3,
329 respectively. The fraction of $Fe(III)_{(oxal)}$ in $Fe_{(oxal)}$ then decreased to 40 % at 10 – 12 cm depth
330 at both sites. Acid volatile sulfur (AVS) exhibited a slight increase with depth at M1 from 0.8
331 µmol cm^{-3} at the surface to 7.2 µmol cm^{-3} at 20 cm depth (Fig. 2E), but was not detected at
332 D3 (Fig. 2J). Concentrations of chromium reducible sulfur (CRS) at M1 increased rapidly
333 with depth from 1.9 µmol cm^{-3} at 0 – 0.5 cm to 21.8 µmol cm^{-3} at 20 cm depth (Fig. 2D),
334 whereas the CRS concentration remained < 0.1 µmol cm^{-3} at D3 (Fig. 2J).
335
336 **3.2 O_2 microprofiles and diffusive oxygen utilization rate**
337
338 Oxygen penetrated less than 4 mm into the sediments (Fig. 3), and rates of diffusive oxygen
339 utilization (DOU) were 7.1 and 6.0 mmol O_2 m^{-2} d^{-1} at M1 and D3, respectively (Table 2).
340 Oxygen consumption by aerobic respiration estimated from the O_2 micro-profiles (area I and
341 II in Fig. 3) was higher at the slope site M1 (4.0 mmol O_2 m^{-2} d^{-1}) than at the D3 in the center
342 of the basin (2.5 mmol O_2 m^{-2} d^{-1}). O_2 consumption by re-oxidation of reduced inorganic
343 compounds indicated by increased activity at the oxic/anoxic interface (area III in Fig. 3)
344 accounted for 43 % and 57 % of the DOU at M1 and D3, respectively. From the profiles of
345 geochemical constituents (Fig. 2), O_2 consumption was mainly attributed to the re-oxidation
346 of sulfide and Fe^{2+} at M1 and of Mn^{2+} at D3.
347
348 **3.3 Anoxic bag incubations**
349
350 Changes in concentrations of DIC, Ca^{2+}, dissolved Mn^{2+} and solid $Fe(II)_{(oxal)}$ over time during
351 anoxic bag incubations from sediment of 0 – 2, 2 – 4, 4 – 6 and 6 – 8 cm depth intervals are
352 presented in Fig. 4. The DIC concentrations increased linearly over time during incubations
353 of sediment in all bags from M1 and D3, except the bag from 6 – 8 cm at D3. The DIC
354 accumulation rates were generally higher at the slope site (M1) than at the basin site (D3)
355 (Table 4). The concentrations of Ca^{2+} decreased with time at all depth intervals of M1,
356 whereas a decrease of Ca^{2+} was observed only for the 2 – 4 cm depth interval at D3. The
357 decrease of Ca^{2+} indicates $CaCO_3$ precipitation, which consequently underestimates DIC
358 accumulation, especially at M1.
359 Coinciding with high concentrations of solid $Mn_{(DCA)}$ (Fig. 2G), prominent Mn^{2+}
360 accumulation appeared at 0 – 6 cm depth of D3, whereas no increase of Mn^{2+} was observed at

Biogeosciences Discuss., doi:10.5194/bg-2016-222, 2016
Manuscript under review for journal Biogeosciences
Published: 3 June 2016

M1 except a slight accumulation at 0 – 2 cm interval (Fig. 4). Solid $Fe(II)_{(oxal)}$ concentrations increased linearly with time at 0 – 4 cm depth of M1, whereas highest $Fe(II)_{(oxal)}$ accumulation was observed at 4 – 6 cm depth at D3. An increase of $Fe(II)_{(oxal)}$ was not discernible in the Mn-oxide-rich surface sediment (0 – 2 cm) of D3.

3.4 Sulfate reduction rates (SRR)

At the slope site (M1), SRR increased from 18 nmol cm^{-3} d^{-1} at the surface to 97 – 103 nmol cm^{-3} d^{-1} at 1.5 – 2 cm depth, and decreased below to 12.5 nmol cm^{-3} d^{-1} at 20 cm depth (Fig. 5B). In contrast, SRR at the manganese oxide-rich basin site (D3) ranged from 1.7 to 8.7 nmol cm^{-3} d^{-1}, and did not vary with depth. Depth integrated SRR down to 10 cm depth was 10 times higher at M1 (4.3 mmol m^{-2} d^{-1}) than at D3 (0.4 mmol m^{-2} d^{-1}) (Table 3).

3.5 DIC production rates

Vertical profiles of the DIC production rate, that were derived from the linear regression of the DIC production measured in anoxic bag incubation (Fig. 4) after correcting for $CaCO_3$ precipitation, are presented in Fig. 5C and 5H for M1 and D3, respectively. At M1, the DIC production rates decreased with depth from 280 nmol cm^{-3} d^{-1} (0 – 2 cm depth) to 69 nmol cm^{-3} d^{-1} (8 – 10 cm depth) (Fig. 5C), whereas the DIC production rates at D3 were relatively similar across the upper 6 cm ranging from 86 to 136 nmol cm^{-3} d^{-1}, and decreased to 8 – 15 nmol cm^{-3} d^{-1} at 6 – 10 cm (Fig. 5H). The integrated DIC production rate within 10 cm depth of the sediment was twice as high at M1 (14.0 mmol m^{-2} d^{-1}) as at the D3 (7.2 mmol m^{-2} d^{-1}) (Table 4).

3.6 Rates of Mn and Fe reduction

The accumulation of Mn^{2+} evidenced that manganese reduction was occurring in the surface sediment (0 – 6 cm) of D3 (Fig. 4). The manganese reduction rate (MnRR) derived from Mn^{2+} accumulation with correction for adsorption ranged from 7.5 nmol cm^{-3} d^{-1} (0 – 2 cm depth) to 198 nmol cm^{-3} d^{-1} (2 – 4 cm depth) at D3 (Fig. 5I). In contrast, MnRR at M1 was indiscernible except for low activity (2.2 nmol cm^{-3} d^{-1}) at 0 – 2 cm depth (Fig. 5D). Depth integrated MnRR at D3 (8.21 mmol m^{-2} d^{-1}) was 200 times higher than the MnRR at M1

Biogeosciences Discuss., doi:10.5194/bg-2016-222, 2016
Manuscript under review for journal Biogeosciences
Published: 3 June 2016

(0.04 mmol m^{-2} d^{-1}) (Table 3). The iron reduction rate (FeRR), derived from $Fe(II)_{(oxal)}$ accumulation, at M1 was highest in the 0 – 2 cm interval (237 nmol cm^{-3} d^{-1}), and then decreased with depth to 38 nmol cm^{-3} d^{-1} at 8 – 10 cm depth (Fig. 5E). In contrast, Fe reduction was not detected in the surface sediment at D3, but increased to its maximum rate of 240 nmol cm^{-3} d^{-1} at 4 – 6 cm depth. The FeRR then decreased with depth to 12 nmol cm^{-3} d^{-1} at 8 – 10 cm (Fig. 5J) where a few data points were adopted to derive the line of best-fit regression. Depth integrated total FeRR was slightly higher at M1 (11.4 mmol m^{-2} d^{-1}) than at D3 (7.53 mmol m^{-2} d^{-1}) (Table 3). The ratio of microbial Fe reduction, $Fe\ Red_{(microbial)}$, to abiotic Fe reduction coupled to sulfide oxidation, $Fe\ Red_{(abiotic)}$, ranged from 1.14 (8 – 10 cm at M1) to 52.3 (2 – 4 cm at D3), which indicated that the Fe reduction at Mn- and Fe oxides rich basin site was mostly a microbiologically mediated process (Table 3).

4 Discussion

4.1 Partitioning of C_{org} oxidation in accordance with the distribution of terminal electron acceptors

One of the most prominent features revealed from the vertical distributions of geochemical constituents at the basin site (D3) was that electron acceptors such as O_2, nitrate, Mn- and Fe oxides were systematically zonated with discrete sequential depletion according to the order of decreasing energy yield for C_{org} oxidation (Fig. 5F). Such biogeochemical zones are not sharply separated in most aquatic sediments due to, e.g., sediment heterogeneity and mixing resulting from bioirrigation, bioturbation, and bottom turbidity currents. The profiles of dissolved and solid phase geochemical constituents in the sediment provide indications as to specific diagenetic reactions prevailing (Froelich et al., 1979). However, reoxidation of reduced inorganic compounds often mask the primary reactions involved in carbon oxidation (Sørensen and Jørgensen, 1987, Hines et al., 1991). Together with the discrete geochemical zonation of the electron acceptors, the independently executed metabolic rate measurements (Fig. 5) allowed us to evaluate the relative contribution of each terminal electron-accepting pathway with sediment depth.

Previous experimental studies that have quantified pathways of anaerobic carbon oxidation in subtidal marine sediments have generally determined the contributions of Mn

Biogeosciences Discuss., doi:10.5194/bg-2016-222, 2016
Manuscript under review for journal Biogeosciences
Published: 3 June 2016

and Fe reduction indirectly from the difference between rates of DIC production and sulfate reduction converted to carbon equivalents (e.g., Canfield et al., 1993b; Thamdrup and Canfield, 1996; Vandieken et al., 2006). The inferred rates of Mn and Fe reduction were further supported by the depth distribution of metal oxides and patterns of Mn^{2+} and Fe^{2+} accumulation in the pore water, but could not be verified because the accumulation of particulate Mn(II) and Fe(II) – which represents the overwhelming fraction of the reduced pools – was not quantified. Here, we combined the indirect approach with independent determination of Mn and Fe reduction rates. Thus, we obtained two separate estimates of anaerobic carbon oxidation rates; based on DIC production and on the sum of sulfate, Fe, and Mn reduction converted to carbon equivalents, respectively (Table 4). At M1, within the 0 – 10 cm depth interval, the average ratio between total anaerobic C_{org} oxidation rate (10.7 mmol C m^{-2} d^{-1}) and the C_{org} oxidation from DIC production (14.0 mmol C m^{-2} d^{-1}) was 0.77 (Table 4). Similarly, at D3, the average ratio between total anaerobic C_{org} oxidation (6.79 mmol m^{-2} d^{-1}) and anaerobic DIC production (7.22 mmol m^{-2} d^{-1}) was 0.94. Consequently, there was a good agreement between the two estimates with a ratio of total anaerobic C_{org} oxidation by Mn + Fe + sulfate : DIC production for individual depth intervals of 0.8 – 1.2 (Table 4) with the exception at the 0 – 2 cm depth of slope site (M1) where the ratio was slightly lower, 0.66, possibly due to a contribution from the C_{org} oxidation by nitrate reduction. The similarity of the two estimates across all incubations spanning a range of redox conditions provides confidence in our approach for calculating dissimilatory Mn and Fe reduction rates. Specifically, the good agreement indicates that the underlying assumptions concerning Mn adsorption and reactions of Fe(III) and sulfide are valid as first-order approximations. The general agreement further supports the validity of previous determinations of dissimilatory Mn and Fe reduction rates based on the difference between DIC production and SO_4^{2-} reduction. (Canfield et al., 1993a, 1993b; Thamdrup et al., 2000; Vandieken et al., 2006; Vandieken et al., 2014).

To elucidate the contribution of sulfate reduction in anaerobic carbon oxidation, the SRRs (Fig. 5B, 5G) were converted to carbon oxidation (Thamdrup and Canfield, 1996), and then compared to the DIC production rates from anoxic bag incubation (Fig. 5C, 5H). At the slope site (M1), the fraction of anaerobic C_{org} oxidation coupled to sulfate reduction increased with depth from 48 % at 0 – 2 cm, to > 90 % at 8 – 10 cm (Table 4). Thus, the excess C_{org} oxidation in the upper layers should be coupled to other electron accepting processes. Indeed, the C_{org} oxidation by Fe reduction (0.96 mmol m^{-2} d^{-1}) accounted for most of the remaining

Biogeosciences Discuss., doi:10.5194/bg-2016-222, 2016
Manuscript under review for journal Biogeosciences
Published: 3 June 2016

anaerobic C_{org} oxidation (11 – 18 % of DIC production) at 0 – 8 cm depth, consistent with the distribution of Fe(III) decreasing from > 25 µmol cm^{-3} near the surface (Fig. 6, Table 4). Mn reduction was of minor importance at M1 because of the low content of Mn oxide (< 3 umol cm^{-3}). Carbon oxidation coupled to aerobic respiration was estimated to 3.1 mmol m^{-2} d^{-1} corresponding to 18 % of the total aerobic + anaerobic oxidation, while the contributions of Fe and sulfate reduction to this total were 12 % and 50 %, respectively (Table 4). As mentioned above, nitrate reduction/denitrification may contribute part of the unexplained 20 % of carbon oxidation, but most of this imbalance likely reflects the combined uncertainties in the estimates of the individual pathways. As discussed further below, the partitioning of C_{org} oxidation at M1 falls within the range previously reported for continental margin sediments.

In contrast to M1, C_{org} oxidation by sulfate reduction at the basin site (D3) accounted for only a small fraction (<10 %) of anaerobic C_{org} oxidation at 0 – 6 cm interval and it only dominated carbon oxidation at 8 – 10 cm (Fig. 5H, Table 4). Oxygen and NO_3^- were depleted within 3.6 mm and 1 cm depth of the sediment surface, respectively (Fig. 5F), while Mn and Fe(III) oxides were abundant at 0 – 4 cm and 0 – 6 cm, respectively. Consistent with the abundance of electron acceptors, high rates of Mn and Fe reduction (Fig. 5I and 5J) implied Mn and Fe reduction as the most significant C_{org} oxidation pathways to 6 cm depth. At 0 – 2 cm depth, C_{org} oxidation by aerobic respiration and Mn reduction accounted for 53 % and 43 % of total C_{org} oxidation, respectively (Fig. 6). At 2 – 4 cm, Mn reduction accounted for 73 % of total C_{org} oxidation and 92 % of anaerobic C_{org} oxidation (Table 4, Fig. 6). Its importance decreased to 22 % at 4 – 6 cm due to lower Mn concentrations, while microbial Fe(III) reduction here contributed 51 %, and the partitioning of sulfate reduction increased to 11 % (Fig. 6). Consequently, the relative distribution of each C_{org} oxidation pathway with depth at D3 (Fig. 6) matched well with the depth distribution of respective electron acceptors (Fig. 5F). Overall, within the 10 cm depth sediments intervals, Mn and Fe reduction were the dominant C_{org} oxidation pathways comprising 45 % and 20 % of total carbon oxidation, respectively, at the Mn and Fe oxide-rich site in the center of the UB (Table 4).

Despite the high Fe oxide content at 0 – 4 cm at D3 (Fig. 5F), no solid $Fe(II)_{(oxal)}$ accumulation was observed at this depth range (Fig. 6). This indicates that Fe(III) reduction may not occur under this Mn-oxide rich conditions. Indeed, using a combination of 16S rRNA-stable isotope probing and geochemical analysis in three manganese oxides-rich sediments including the UB, Vandieken et al. (2012) identified bacteria related to *Colwellia*, *Oceanospillaceae* and *Arcobacter* as acetate-oxidizing bacteria that potentially reduce

Biogeosciences Discuss., doi:10.5194/bg-2016-222, 2016
Manuscript under review for journal Biogeosciences
Published: 3 June 2016

493 manganese, whereas no known iron reducers were detected in the Mn-rich sediment.
494 Similarly, Thamdrup et al. (2000), in Mn oxide- rich Black Sea sediment, found that the
495 abundance of viable Fe-reducing bacteria in most probable number counts was low in
496 comparison to Mn reducers and the addition of ferrihydrite did not stimulate Fe reduction,
497 which implied that Fe reduction should be outcompeted by the Mn reduction process.

498 Nonetheless, Mn reduction estimated from the increase of Mn^{2+} at 0 – 4 cm interval at D3
499 (Fig. 6) could be due to oxidation of Fe^{2+} or sulfide. Fe^{2+} may readily react with Mn oxides
500 (Myers and Nealson, 1988; Lovley and Phillips, 1988) by the reaction $2Fe^{2+} + MnO_2 + 4H_2O$
501 $= Mn^{2+} + 2Fe(OH)_3 + 2H^+$. However, in the Mn oxide-rich sediment of the Skagerrak,
502 Canfield et al. (1993b) revealed that the addition of Ferrozine, a strong complexation agent
503 for Fe^{2+}, had no inhibitory effect on the Mn^{2+} liberation, indicating that the chemical reaction
504 of MnO_2 with Fe^{2+} generated by Fe reduction was not responsible for the accumulation of
505 Mn^{2+}. As manganese reduction is thermodynamically more favorable than iron and sulfate
506 reduction, the Mn^{2+} liberation (Fig. 3) likely resulted from dissimilatory Mn reduction.

507 Despite anoxia and nitrate depletion, Mn reduction rates at 0 – 2 cm depth (Fig. 5I) based
508 on Mn^{2+} accumulation were substantially lower than the rates inferred from DIC
509 accumulation (Fig. 5H). A similar discrepancy was previously observed for the uppermost
510 part of the Mn reduction zone (Thamdrup et al., 2000), and is likely explained by particularly
511 strong sorption of Mn^{2+} to fresh Mn oxide surfaces, which is not included in the adsorption
512 coefficient used here. Previous estimation of denitrification in 0 – 2 cm depth of the UB
513 ranged from 0.01 to 0.17 mmol N m^{-2} d^{-1} (Lee, 2009), which is equivalent to a C_{org} oxidation
514 of 0.013 – 0.213 mmol C m^{-2} d^{-1} using the stoichiometric equation of $4H^+ + 5CH_2O + 4NO_3^-$
515 $= 5CO_2 + 2N_2 + 7H_2O$. Based on the average, the contribution of carbon oxidation by
516 denitrification (0.11 mmol C m^{-2} d^{-1}) should be minor at the basin site (≤ 3 % of total C_{org}
517 oxidation at 0 – 2 cm; ~1 % of integrated C_{org} oxidation). This is consistent with the general
518 consensus that C_{org} oxidation by denitrification is of little importance in most marine
519 sediments (Sørensen et al., 1979; Canfield et al., 1993a; Trimmer and Engström, 2011).
520 Denitrification may be even further suppressed in Mn-rich sediments due to competitive
521 inhibition from Mn reduction (Trimmer et al., 2013).

522

523 **4.2 C_{org} oxidation dominated by manganese reduction in the UB**

524

525 Microbial Fe reduction has been quantified directly in sediments of various coastal oceans

Biogeosciences Discuss., doi:10.5194/bg-2016-222, 2016
Manuscript under review for journal Biogeosciences
Published: 3 June 2016

(Gribsholt et al., 2003; Kostka et al., 2002a, 2002b; Hyun et al., 2007, 2009b) and indirectly in deeper continental margins (Thamdrup and Canfield, 1996; Jensen et al., 2003; Kostka et al., 1999). Earlier estimation from 16 different continental margin sediments indicated that Fe(III) reduction contributed 22 % on average to anaerobic carbon oxidation (Thamdrup, 2000). Thus, the contributions from Fe(III) reduction of 12 % and 20 % of anaerobic C_{org} oxidation on the slope (M1) and in the basin (D3) of the UB (Table 4) falls in the range of the previous indirect estimates.

Unlike Fe reduction, direct estimation of manganese reduction rates is not easy, mainly because of the restriction of the process to a thin surface layer (Sundby and Silverberg, 1985), the rapid reduction of manganese oxides with H_2S and Fe^{2+} (Postma, 1985; Burdige and Nealson, 1986; Kostka et al., 1995; Lovley and Phillips, 1988), and the adsorption of Mn^{2+} to Mn oxide surface (Canfield et al., 1993b). For that reason, only two studies, from the Skagerrak and Black Sea, are available for direct comparison on the partitioning of Mn reduction. The process has also been indicated to be of importance in the Panama Basin based on diagenetic modeling (Aller, 1990) and at some Artic shelf sites where it was however not quantified separately from Fe reduction (Vandieken et al., 2006, Nickel et al., 2008). Mn reduction was responsible for over 90 % of total C_{org} oxidation at 600 m depth in the Skagerrak, and accounted for 13 – 45 % of anaerobic C_{org} oxidation in the Black Sea shelf sites at 60 – 130 m of water depth. To our knowledge, this report of C_{org} oxidation dominated by Mn reduction comprising 45 % of total C_{org} oxidation and 57 % of anaerobic C_{org} respiration in the center of the UB (Table 4) represents the first from deep-offshore basin of the eastern Asian marginal seas.

The difference in partitioning of Mn reduction in C_{org} oxidation between the UB, Black Sea and Skagerrak reflects the close relationship between Mn oxide content in the sediment and Mn reduction (Thamdrup et al., 2000). From the vertical distribution of electron acceptors (Fig. 5J) and contribution of each C_{org} oxidation pathway with depth (Fig. 6), it is apparent that the availability of Mn(IV) largely controls the relative contribution to C oxidation. In the Skagerrak, the Mn oxides are abundant in high concentration down to 10 cm depth (Canfield et al., 1993b), whereas Mn oxides in the Black Sea and the Ulleung Basin were enriched only down to 2 cm and 4 cm, respectively (Thamdrup et al., 2000, Fig. 2). Using the available data set for the three marine sediments, we further plotted the relative contribution of manganese reduction to total carbon oxidation as a function of Mn-oxides concentration to expand data from Thamdrup et al., 2000 (Fig. 7). The plot indicates

Biogeosciences Discuss., doi:10.5194/bg-2016-222, 2016
Manuscript under review for journal Biogeosciences
Published: 3 June 2016

559 saturation kinetics with a close correlation between Mn oxide content and the importance of
560 Mn reduction at low concentrations. Curve-fitting yields a concentration of MnO_2 at 50 % of
561 contribution of manganese reduction to total C_{org} oxidation (K_s) of 8.6 µmol cm^{-3} similar to
562 the approx. 10 µmol cm^{-3} suggested before (Thamdrup et al., 2000). This indicates that Mn
563 reduction can be a dominant C_{org} oxidation process even at low concentrations of Mn oxides
564 compared to those found at UB. Manganese enrichments of this magnitude have been
565 reported for several locations on the continental margins (Murray et al., 1984; Gobeil et al.,
566 1997; Haese et al., 2000; Mouret et al., 2009; Magen et al., 2011; Macdonald and Gobeil,
567 2012) in addition to the relatively few places where dissimilatory Mn reduction was already
568 indicated to be of importance, as discussed above. Thus, the process may be of more
569 widespread significance on continental margins.
570
571 **4.3 Source of high Mn oxide content**
572
573 The strong enrichment of Mn in the UB surface sediment is primarily of diagenetic origin as
574 indicated by similar Mn concentrations at depth in the sediment at D3 (0.95 – 3.02 µmol cm^{-3})
575 compared to M1 (0.36 – 3.74 µmol cm^{-3}) (Fig. 2) combined with higher sediment
576 accumulation rates at the slope (0.15 – 0.3 cm y^{-1}) than in the basin (0.07 cm y^{-1}; Cha et al.,
577 2005). Thus, the burial flux of Mn, and thereby the net input assuming steady state deposition,
578 is higher at M1 than at D3. Furthermore, Mn is likely subject to geochemical focusing in the
579 basin as Mn depositing at shallower depths is reductively mobilized and incompletely
580 oxidized in the thin oxic surface layer, resulting in release to the water column and net down-
581 slope transport, as inferred in other ventilated basins (Sundby and Silverberg, 1985; Canfield
582 at al., 1993b). A diagenetic source of Mn enrichment was also concluded in previous studies
583 (Yin et al., 1989; Cha et al., 2007; Choi et al., 2009). The Mn remaining and being buried at
584 M1 likely represents unreactive detrital forms to a larger extent than at D3 (Cha et al., 2007).
585 Adopting the sediment accumulation rate of 0.07 cm y^{-1} in the UB determined at a station 50
586 km from D3 (Cha et al., 2005), the average $Mn_{(DCA)}$ concentration of 1.1 µmol cm^{-3} at 10 –
587 20 cm depth (Fig. 2G) corresponds to a flux for permanent burial of 0.002 mmol m^{-2} d^{-1} or
588 just 0.03 % of the Mn reduction rate (Table 3), i.e., an Mn atom is recycled 3800 times before
589 it finally gets buried. This is a much more extensive recycling than found in the Mn sediment
590 of Skagerrak (130 – 260 times; Canfield et al., 1993b). The difference results mainly from a
591 much higher burial flux of Mn (as authigenic Mn[II]) in the Skagerrak (~40 µmol cm^{-3};

Biogeosciences Discuss., doi:10.5194/bg-2016-222, 2016
Manuscript under review for journal Biogeosciences
Published: 3 June 2016

592 Canfield et al., 1993b). The reason that little, if any, authigenic Mn(II) is buried in the UB is
593 not clear.

594 As noted in previous studies (Aller 1990, Canfield et al. 1993b), high contributions of Mn
595 and Fe reduction to carbon oxidation in off-shore sediments requires physical mixing, which
596 typically occurs through bioturbation. This is also the case for the UB, where the burial flux
597 from the oxic surface layer into the Mn reduction zone corresponded to 0.4 mmol m^{-2} d^{-1} or 5 %
598 of the Mn reduction rate (213 µmol cm^{-3} x 0.07 cm y^{-1}). Bioturbation has previously been
599 inferred, but not quantified, from ^{210}Pb profiles in the UB (Cha, 2002), and thin polychaete
600 worms were observed during our sampling. Assuming bioturbation to be a diffusive process,
601 we estimate, in a similar manner as in the previous studies and based on the average gradient
602 in $Mn_{(DCA)}$ from 0.5 – 1 to 7 – 8 cm, that the Mn reduction rate would be supported at a
603 biodiffusion coefficient of 9.5 cm^2 y^{-1}. This value is 3.6 times lower than the coefficient
604 estimated for the Skagerrak (Canfield et al., 1993b) and consistent with estimates for other
605 sediments with similar deposition rates (Boudreau, 1994). Thus, it is realistic that
606 bioturbation drives Mn cycling in the UB.

607
608
609 **4.4 The UB as a biogeochemical hotspot**
610
611 The SRRs measured in this study (0.43 – 4.29 mmol m^{-2} d^{-1}) are higher than those of
612 measured in productive systems such as the Benguela upwelling system in the Southeast
613 Atlantic (Ferdelman et al., 1999; Fossing et al., 2000), and even comparable to those reported
614 at the continental slope of the Chilean upwelling system (2.7 – 4.8 mmol m^{-2} d^{-1}) (Thamdrup
615 and Canfield, 1996) at a similar depth range of 1000 – 2500 m. The total anaerobic DIC
616 production rates at the slope (14.0 mmol m^{-2} d^{-1}) and basin site (7.2 mmol m^{-2} d^{-1}) were also
617 comparable to those measured at the same depth range of Chilean upwelling site (9.2 – 11.6
618 mmol m^{-2} d^{-1}) (Thamdrup and Canfield, 1996). Since rates of benthic carbon oxidation are
619 largely controlled by the supply of organic carbon (Canfield et al., 2005), a high organic flux
620 reflected in the high organic content (> 2.5 %, dry wt.) in the sediment of the UB (Table 1) is
621 likely to explain the high metabolic activities. A similar high organic carbon content as in the
622 UB is rarely found in deep-sea sediment underlying oxic bottom water at depths exceeding
623 2000 m, except for Chilean upwelling site (Lee et al., 2008). This high organic carbon
624 content in the UB is mainly associated with the combination of enhanced biological
625 production resulting from the formation of coastal upwelling (Hyun et al., 2009a), occurrence

Biogeosciences Discuss., doi:10.5194/bg-2016-222, 2016
Manuscript under review for journal Biogeosciences
Published: 3 June 2016

of an intrathermocline eddy resulting in the extraordinary subsurface chlorophyll-a maximum (Kim et al., 2012), high organic C accumulation rates exceeding 2 g C m^{-2} yr^{-1} (Lee et al., 2008), and high export production (Kim et al., 2009). In addition to the large vertical sinking flux, the lateral transport of the organic matter along the highly productive southeastern slope of the UB also contributes to the high organic content (Lee et al., 2015). Consequently, high benthic mineralization resulting from the high organic content in the sediment implied that the UB is a biogoechemical hotspot where significant turnover of organic matter and nutrient regeneration occur. Recently, a rapid increase of sea surface temperature of 1.09 ℃ in the East Sea over the last two decades (1982 – 2006) has been recorded, which is the fourth highest among the 18 large marine ecosystems in the world ocean (Belkin, 2009). It is thus important to monitor any changes in the rates and partitioning of C_{org} oxidation to better understand the biogeochemical carbon, nutrients and metal cycles associated with long-term climatic changes in the UB, the biogeochemical hotspot of the East Sea.

5. Conclusions

Surface sediments of the Ulleung Basin (UB) in the far east Eurasian continent are characterized by a high organic carbon content (> 2.5 %, dry wt.) high concentrations Fe oxides (up to 100 μmol cm^{-3}), and very high concentrations of Mn oxides (> 200 μmol cm^{-3}). For the first time in the Asian marginal seas, and in one of only few experimental studies of the partitioning of C_{org} oxidation pathways in deep-sea sediments in general, we show that microbial Mn and Fe reduction are the dominant C_{org} oxidation pathways, comprising 45 % and 20 % of total C_{org} oxidation, respectively. The high Mn content results from highly efficient recycling through reoxidation with very low permant burial of authigenic Mn(II) phases. The basin topography may ensure that any Mn^{2+} escaping to the overlying water returns to the sediment after reprecipitation. The relative importance of Mn reduction to C_{org} oxidation displays saturation kinetics with respect to Mn oxide content with a low half-saturation value (8.6 μmol cm^{-3}), which further implies that Mn reduction can be a dominant C_{org} oxidation process in sediments with lower MnO_2 content, and thereby that the process might be more important in deep-sea sediments than previously thought. Vertical distributions of the major terminal electron acceptors such as O_2, nitrate, Mn- and Fe oxides were systematically zonated with discrete sequential depletion according to the order of

Biogeosciences Discuss., doi:10.5194/bg-2016-222, 2016
Manuscript under review for journal Biogeosciences
Published: 3 June 2016

659 decreasing energy yield for C_{org} oxidation, which are not sharply separated in most aquatic
660 sediments due to, e.g., sediment heterogeneity and mixing resulting from bioirrigation,
661 bioturbation, and bottom turbidity currents. High benthic mineralization resulting from the
662 high organic carbon content in the sediment implied that the UB is a biogoechemical hotspot
663 where significant turnover of organic matter and nutrient regeneration occur. The East Sea,
664 including the UB, has experienced the fastest increase in sea water temperature (1.09 ^{o}C) for
665 the past two decades (1982 – 2006). If this continues, the UB sediment provides with an ideal
666 natural laboratory to monitor changes in the rates and partitioning of C_{org} oxidation in order
667 to better understand the biogeochemical cycling of carbon, nutrients and metals associated
668 with long-term climatic changes.
669
670

671 ## Author contribution
672

673 J-H Hyun as first author and leader of the Korean research group designed the original
674 experiments and conducted most writing; S-H Kim, JS Mok, and H-Y Cho participated in
675 onboard research activities and analytical processes; V Vandieken participated in onboard
676 research and was actively involved in the discussion of the manuscript; D Lee, as project
677 manager of the EAST-1 program, paid the ship-time and has participated in discussion of the
678 results; B Thamdrup, as leader of the Danish research group, collaborated with J-H Hyun in
679 designing the experiments and writing and discussing the manuscript.
680

681

682 ## Acknowledgements

683 This research was a part of the projects titled Korean Long-term Marine Ecological
684 Researches (K-LTMER) and East Asian Seas Time Series-I (EAST-I) funded by the Korean
685 Ministry of Oceans and Fisheries, and was also supported by the National Research
686 Foundation of Korea (NRF-2012-013-2012S1A2A1A01030760) in collaboration with the
687 Danish Council for Independent Research and the Danish National Research Foundation
688 (DNRF53).

689

Biogeosciences Discuss., doi:10.5194/bg-2016-222, 2016
Manuscript under review for journal Biogeosciences
Published: 3 June 2016

690

691 ## References

692

693 Aller, R. C. : Bioturbation and manganese cycling in hemipelagic sediments, Phil. Trans. R.
694 Soc. Lond. A 331, 51-68, 1990.
695 Belkin, I. M. : Rapid warming of Large Marine Ecosystems, Prog. Oceanogr., 81, 207-213,
696 2009.
697 Berg, P., Risgaard-Petersen, N., and Rysgaard, S. : Interpretation shelf and slope: A
698 comparison of *in situ* microelectrode and chamber flux measurements, Limnol. Oceanogr.,
699 37**,** 614-629, 1998.
700 Boudreau, B. P. : Is burial velocity a master parameter for bioturbation?, Geochim.
701 Cosmochim. Acta, 58, 1243-1249, 1994.
702 Burdige, D. J. and Nealson, K. H., : Chemical and microbiological studies of sulfide-
703 mediated manganese reduction, Geomicrobiol. J., 4, 361-387, 1986.
704 Canfield, D. E., Jørgensen, B. B., Fossing, H., Glud, R., Gundersen, J., Rasing, N. B.,
705 Thamdrup, B., Hansen, J. W., Nielsen, L. P., and Hall, P. O. J. : Pathways of organic
706 carbon oxidation in three continental margin sediments, Mar. Geol., 113, 27-40, 1993a.
707 Canfield, D. E., Thamdrup, B., and Hansen, J. W. : The anaerobic degradation of organic
708 matter in Danish coastal sediments: iron reduction, manganese reduction, and sulfate
709 reduction, Geochim. Cosmochim. Acta 57, 3867-3883, 1993b.
710 Canfield, D. E., Thamdrup, B., and Kristensen, E. (Eds.) : Aquatic geomicrobiology, Elsevier,
711 San Diego, 640 pp., 2005.
712 Cha, H. J. : Geochemistry of surface sediments and diagenetic redistribution of phosphorus in
713 the southwestern East Sea, PhD thesis, Seoul National Univ., Seoul, Korea, 190 pp., 2002.
714 Cha, H. J., Choi, M. S., Lee, C.-B., and Shin, D.-H. : Geochemistry of surface sediments in
715 the southwestern East/Japan Sea, J. Asian Earth Sci., 29, 685-697, 2007.

Biogeosciences Discuss., doi:10.5194/bg-2016-222, 2016
Manuscript under review for journal Biogeosciences
Published: 3 June 2016

716 Cha, H. J., Lee, C. B., Kim, B. S., Choi, M. S., and Ruttenberg, K. C. : Early diagenetic
717 redistribution and burial of phosphorus in the sediments of the southwestern East Sea
718 (Japan Sea), Mar. Geol., 216, 127-143, 2005.
719 Choi, Y. J., Kim, D. S., Lee, T. H., and Lee, C. B. : Estimate of manganese and iron oxide
720 reduction rates in slope and basin sediments of Ulleung Basin, East Sea, J. Korean Soc.
721 Oceanogr., 14, 127-133, 2009.
722 Cline, J. D. : Spectrophotometric determination of hydrogen sulfide in natural waters, Limnol.
723 Oceanogr., 14, 454-458, 1969.
724 Fossing, H., Ferdelman, T. G., and Berg, P. : Sulfate reduction and methane oxidation in
725 continental margin sediments influenced by irrigation (South-East Atlantic off Namibia),
726 Geochim. Cosmochim. Acta, 64, 897-910, 2000.
727 Fossing, H. and Jørgensen, B. B. : Measurement of bacterial sulfate reduction in sediments:
728 evaluation of a single-step chromium reduction method, Biogeochem. 8, 205-222, 1989.
729 Ferdelman, T. G., Fossing, H., Neumann, K., and Schulz, H. D. : Sulfate reduction in surface
730 sediments of the southeast Atlantic continental margin between 15°38´S and 27°57´S
731 (Angola and Namibia), Limnol. Oceanogr., 44, 650-661, 1999.
732 Froelich, P. N., Klinkhammer, G. P., Bender, M. L., Luedtke, N. A., Heath, G. R., Cullen, D.,
733 Dauphin, P., Hammond, D., Hartman, B., and Maynard, V. : Early oxidation of organic
734 matter in pelagic sediments of the eastern equatorial Atlantic: suboxic diagenesis,
735 Geochim. Cosmochim. Acta, 43, 1075-1090, 1979.
736 Glud, R. N. : Oxygen dynamics of marine sediments, Mar. Biol. Res., 4, 243-289, 2008.
737 Gobeil, C, Macdonald, R. W., and Sundby, B. : Diagenetic separation of cadmium and
738 manganese in suboxic continental margin sediments, Geochim. Cosmochim. Acta, 61,
739 4647-4654, 1997.
740 Gribsholt, B., Kostka, J. E., and Kristensen, E. : Impact of fiddler crabs and plant roots on

741 sediment biogeochemistry in a Georgia saltmarsh, Mar. Ecol. Prog. Ser., 259, 237-251,
742 2003.
743 Haese, R. R., Schramm, J., Rutgers Van Der Loeff, M. M., and Schult, H. D. : A comparative
744 study of iron and manganese diagenesis in continental slope and deep sea basin sediments
745 off Uruguay (SW Atlantic), Int. J. Earth Sci., 88, 619-629, 2000.
746 Hall, P. O. and Aller, R.C. : Rapid small-volume, flow injection analysis for CO_2 and NH_4^+ in
747 marine and freshwaters, Limnol. Oceanogr., 37, 113-119, 1992.
748 Hansen, J. W., Thamdrup, B., and Jørgensen, B. B. : Anoxic incubation of sediment in gas-
749 tight plastic bags: a method for biochemical process studies, Mar. Ecol. Prog. Ser., 208,
750 273-282, 2000.
751 Hines, M. E., Bzylinski, D. A., Tugel, J. B., and Lyons, W. B. : Anaerobic microbial
752 biogeochemistry in sediments from two basins in the Gulf of Maine: evidence for iron and
753 manganese reduction, Estuar. Coast. Shelf Sci., 32, 313-324, 1991.
754 Hyun, J.-H., Smith, A. C., and Kostka, J. E. : Relative contributions of sulfate- and iron(III)
755 reduction to organic matter mineralization and process controls in contrasting habitats of
756 the Georgia saltmarsh, Appl. Geochem., 22, 2637-2651, 2007.
757 Hyun, J.-H., Kim, D., Shin, C.-W., Noh, J.-H., Yang, E.-J., Mok, J.-S., Kim, S.-H., Kim, H.-
758 C., and Yoo, S. : Enhanced phytoplankton and bacterioplankton production coupled to
759 coastal upwelling and an anticyclonic eddy in the Ulleung basin, East Sea, Aquat. Microb.
760 Ecol., 54, 45–54, 2009a.
761 Hyun, J.-H., Mok, J.-S., Cho, H.-Y., Kim, S.-H., and Kostka, J. E. : Rapid organic matter
762 mineralization coupled to iron cycling in intertidal mud flats of the Han River estuary,
763 Yellow Sea, Biogeochem., 92, 231-245, 2009b.

764 Hyun, J.-H., Mok, J.-S., You, O.-R., Kim, D., and Choi, D. L. : Variations and controls of
765 sulfate reduction in the continental slope and rise of the Ulleung basin off the southeast
766 Korean upwelling system in the East Sea, Geomicrobiol. J., 27, 1-11, 2010.
767 Jahnke, R. A., Emerson, S. R., and Murray, J. W. : A model of oxygen reduction,
768 denitrification, and organic matter mineralization in marine sediments, Limnol. Oceanogr.,
769 27, 610-623, 1982.
770 Jahnke, R. A., Reimers, C. E., and Craven, D. B. : Intensification of recycling of organic
771 matter at the sea floor near ocean margins, Nature, 348, 50-54, 1990.
772 Jahnke, R. A. and Jahnke, D. B. : Rates of C, N, P and Si recycling and denitrification at the
773 US mid-Atlantic continental slope depocenter, Deep-Sea Res. I, 47, 1405-1428, 2000.
774 Jensen, M. M., Thamdrup, B., Rysgaard, S., Holmer, M., and Fossing, H. : Rates and
775 regulation of microbial iron reduction in sediments of the Baltic–North Sea transition,
776 Biogeochem., 65, 295-317, 2003.
777 Jørgensen, B. B. : A comparison of methods for the quantification of bacterial sulfate
778 reduction in coastal marine sediments, 1. Measurement with radiotracer techniques,
779 Geomicrobiol. J., 1, 11–28, 1978.
780 Jørgensen, B. B. : Mineralization of organic matter in the sea bed - the role of sulphate
781 reduction, Nature, 296, 643-645, 1982.
782 Jørgensen, B. B. and Revsbech, N. P. : Diffusive boundary layers and the oxygen uptake of
783 sediments and detritus, Limnol. Oceanogr., 30, 111-122, 1985.
784 Jørgensen, B. B. : Bacteria and marine biogeochemistry, in: Marine Geochemistry, edited by:
785 Schulz, H. D. and Zabel, M., Springer-Verlag, Berlin, Heidelberg, NY, 169-206, 2006.
786 Jørgensen, B. B. and Kasten, S. : Sulfur cycling and methane oxidation. in: Marine
787 Geochemistry, edited by: Schulz, H. D. and Zabel, M., Springer-Verlag, Berlin,
788 Heidelberg, NY, 271-309, 2006.

Biogeosciences Discuss., doi:10.5194/bg-2016-222, 2016
Manuscript under review for journal Biogeosciences
Published: 3 June 2016

789 Kim, D., Choi, M.-S., Oh, H.-Y., Kim, K. H., and Noh, J.-H. : Estimate of particulate organic
790 carbon export flux using $^{234}Th/^{238}U$ disequilibrium in the southwestern East Sea during
791 summer, (The Sea) J. Kor. Soc. Oceanogr., 14, 1-9, 2009.
792 Kim, D., Yang, E.J., Kim, K. H., Shin, C.-W., Park, J., Yoo, S. J., and Hyun, J.-H. : Impact of
793 an anticyclonic eddy on the summer nutrient and chlorophyll a distributions in the Ulleung
794 Basin, East Sea (Japan Sea), ICES J. Marine Science, 69, 23-29, 2012.
795 Kostka, J. E., Luther, G. W., and Nealson, K. H. : Chemical and biological reduction of
796 Mn(III)-pyrophosphate complexes – potential importance of dissolved Mn(III) as an
797 environmental oxidant, Geochim. Cosmochim. Acta, 59, 885-894, 1995.
798 Kostka, J. E., Thamdrup, B., Glud, R. N., and Canfield, D. E. : Rates and pathways of carbon
799 oxidation in permanently cold Arctic sediments, Mar. Ecol. Prog. Ser. 180, 7-21, 1999.
800 Kostka, J. E., Gribsholt, B., Petrie, E., Dalton, D., Skelton, H., and Kristensen, E. : The rates
801 and pathways of carbon oxidation in bioturbated saltmarsh sediments, Limnol.
802 Oceanogr .47, 230-240, 2002a.
803 Kostka, J. E., Roychoudhury, A., and Van Cappellen, P. : Rates and controls of anaerobic
804 microbial respiration across spatial and temporal gradients in saltmarsh sediments,
805 Biogeochem, 60, 49–76, 2002b.
806 Lee, T., Hyun, J.-H., Mok, J. S., and Kim, D. : Organic carbon accumulation and sulfate
807 reduction rates in slope and basin sediments of the Ulleung basin, East/Japan Sea, Geo.
808 Mar. Lett. 28, 153-159, 2008.
809 Lee, J. : Importance of nitrate reduction in coastal and deep-sea sediments, MS thesis,
810 Department of Marine Science Graduate School, Pusan National University, Korea, 86 pp.,
811 2009.
812 Lee, J. S., An, S.-U., Park, Y.-G., Kim, E., Kim, D., Kwon, J. N., Kang, D.-J., and Noh, J.-H. :
813 Rates of total oxygen uptake of sediments and benthic nutrient fluxes measured using an

Biogeosciences Discuss., doi:10.5194/bg-2016-222, 2016
Manuscript under review for journal Biogeosciences
Published: 3 June 2016

in situ autonomous benthic chamber in the sediment of the slope off the southwestern part of the Ulleung Basin, East Sea, Ocean Sci. J., 50, 581-588, 2015.

Li, Y. H. and Gregory, S. : Diffusion of ions in sea water and deep sea sediments. Geochim. Cosmochim. Acta, 38, 703-714, 1974.

Lovley, D. R. and Phillips, E. J. P. : Competitive mechanisms for inhibition of sulfate reduction and methane production in the zone of ferric iron reduction in sediments, Appl. Environ. Microbiol., 53, 2636-2641, 1987.

Lovley, D. R. and Phillips, E. J. P. : Manganese inhibition of microbial iron reduction in anaerobic sediments, Geomicrobiol. J., 6, 145-155, 1988.

Macdonald, R. W. and Gobeil, C. : Manganese sources and sinks in the Arctic Ocean with reference to periodic enrichments in basin sediments, Aquat. Geochem., 18, 565-591, 2012.

Magen, C., Mucci, A., and Sundby, B. : Reduction rates of sedimentary Mn and Fe oxides: an incubation experiment with Arctic Ocean sediments, Aquat. Biogeochem., 17, 629-643, 2011.

Meyers, C. and Nealson, K. H. : Microbial reduction of manganese oxides: Interactions with iron and sulfur, Geochim. Cosmochim. Acta, 52, 2727-2732, 1988.

Mouret, A., Anschutz, P., Lecroart, P., Chaillou, G., Hyacinthe, C., Deborde, J., Jorissen, F., Deflandre, B., Schmidt, S., and Jouanneau, J.-M. : Benthic geochemistry of manganese in the Bay of Biscay, and sediment mass accumulation rate, Geo. Mar. Lett. 29, 133-149, 2009.

Murray, J. W., Balistrieri, L. S., and Paul, B. : The oxidation state of manganese in marine sediments and ferromanganese nodules, Geochim. Cosmochim. Acta, 48, 1237-1247, 1984.

Nickel, M., Vandieken, V., Brüchert, V., and Jørgensen, B. B. : Microbial Mn(IV) and Fe(III) reduction in northern Barents Sea sediments under different conditions of ice cover and organic carbon deposition, Deep-Sea Res. II, 55, 2390-2398, 2008.

839 Parsons, T. R., Maita, Y., and Lalli, C. M. (Eds.) : A manual of chemical and biological
840 methods for seawater analysis, Pergamon Press, Oxford, 173 pp., 1984.
841 Phillips, E. J. P. and Lovley, D. R. : Determination of Fe(III) and Fe(II) in oxalate extracts of
842 sediment, Soil Sci. Soc. Am. J., 51, 938-941, 1987.
843 Postma, D. : Concentration of Mn and separation from Fe in sediments – I. Kinetics and
844 stoichiometry of the reaction between birnessite and dissolved Fe(II) at 10°C, Geochim.
845 Cosmochim. Acta, 49, 1023-1033, 1985.
846 Pyzik, A. E. and Sommer, S. E. : Sedimentary iron monosulfide: kinetics and mechanisms of
847 formation, Geochim. Cosmochim. Acta, 45, 687-698, 1981.
848 Rasmussen, H. and Jørgensen, B. B. : Microelectrode studies of seasonal oxygen uptake in a
849 coastal sediment: role of molecular diffusion, Mar. Ecol. Prog. Ser., 81, 289-303, 1992.
850 Romankevich, E. A. : Geochemistry of organic matter in the ocean, Springer-Verlag, Berlin,
851 Heidelberg, NY, Tokyo, 334 pp., 1984.
852 Sørensen, J. W. and Jørgensen, B. B. : Early diagenesis in sediments from Danish coastal
853 waters: Microbial activity and Mn-Fe-S geochemistry, Geochim. Cosmochim. Acta, 51,
854 1583-1590, 1987.
855 Sørensen, J. W., Jørgensen, B. B., and Revsbech, N. P. : A comparison of oxygen, nitrate and
856 sulfate respiration in a coastal marine sediment, Microb. Ecol., 5, 105-115, 1979.
857 Stookey, L. L. : Ferrozine - a new spectrophotometric reagent for iron, Anal. Chemi. 42, 779-
858 781, 1970.
859 Sundy, B. and Silverberg, N. : Manganese fluxes in the benthic boundary layer, Limnol.
860 Oceanogr., 30, 372-381, 1985.
861 Thamdrup, B. : Bacterial manganese and iron reduction in aquatic sediments, Adv. Microb.
862 Ecol. 16, 41-84, 2000.
863 Thamdrup, B. and Canfield, D. E. : Pathways of carbon oxidation in continental margin

sediments off central Chile, Limnol. Oceanogr. 41, 1629-1650, 1996.

Thamdrup, B. and Dalsgaard, T. : The fate of ammonium in anoxic manganese oxide-rich marine sediment, Geochim. Cosmochim. Acta, 64, 4157-4164, 2000.

Thamdrup, B., Rosselló-Mora, R., and Amann, R. : Microbial manganese and sulfate reduction in Black Sea shelf sediments, Appl. Environ. Microbiol., 66, 2888-2897, 2000.

Trimmer, M. and Engström, P. : Distribution, activity, and ecology of anammox bacteria in aquatic environments, in: Nitrification, edited by: Ward, B. B., Arp, D. J., and Klotz, M. G., ASM Press, Washington, DC, 201-235, 2011.

Trimmer, M., Engström, P., and Thamdrup, B. : Stark contrast in denitrification and anammox across the deep Norwegian Trench in the Skagerrak, Appl. Environ. Microbiol., 79, 7381-7389, 2013.

Vandieken, V., Finke, N., and Thamdrup, B. : Hydrogen, acetate, and lactate as electron donors for microbial manganese reduction in a manganese-rich coastal marine sediment, FEMS Micribiol Ecol., 87, 733-745, 2014.

Vandieken, V., Nickel, M., and Jørgensen, B. B. : Carbon mineralization in Arctic sediments northeast of Svalbard: Mn(IV) and Fe(III) reduction as principal anaerobic respiratory pathways, Mar. Ecol. Prog. Ser., 322, 15-27, 2006.

Vandieken, V, Pester, M., Finke, N., Hyun, J.-H., Friedrich, M.W., Loy, A., and Thamdrup, B. : Identification of acetate-oxidizing manganese-reducing bacteria in three manganese oxide-rich marine sediments by stable isotope probing, ISME J., 6, 2078-2090, 2012.

Walsh, J. J. : Importance of continental margins in the marine biogeochemical cycling of carbon and nitrogen, Nature, 350, 53-55, 1991.

Yamada, K., Ishizaka, J., and Nagata, H. : Spatial and temporal variability of satellite primary production in the Japan Sea from 1998 to 2002, J. Oceanogr., 61, 857-869, 2005.

Biogeosciences Discuss., doi:10.5194/bg-2016-222, 2016
Manuscript under review for journal Biogeosciences
Published: 3 June 2016

888 Yin, J. H., Kajiwara, Y., and Fujii, T. : Distribution of transition elements in surface
889 sediments of the southwestern margin of Japan Sea. Geochem. J., 23, 161-180, 1989.
890 Yoo, S. and Park, J. S. : Why is the southwest the most productive region of the East Sea/Sea
891 of Japan?, J. Mar. Syst., 78, 301-315, 2009.
892

Biogeosciences Discuss., doi:10.5194/bg-2016-222, 2016
Manuscript under review for journal Biogeosciences
Published: 3 June 2016

893

894 Table 1. Environmental settings and sediment characteristics

Environmental parameter	M1 (Continental slope)	D3 (Center of the basin)
Latitude	36° 10' N	37° 00' N
Longitude	130° 10' E	131° 00' E
Water depth (m)	1,453	2,154
Sediment temperature (°C)	1.3	0.6
Pore-water salinity (psu)	34.2	34.8
Water content (%)	85 (± 3.1)	77 (± 1.8)
Porosity	0.95 (± 0.03)	0.86 (± 0.01)
Density (g cm^{-3})	1.10 (± 0.02)	1.12 (± 0.02)
Total organic carbon (%, dry wt.)	3.96 (± 0.27)	2.66 (± 0.09)
Total organic nitrogen (%, dry wt.)	0.38 (± 0.01)	0.35 (± 0.01)

895 Numbers in parenthesis indicate ± 1SD of triplicate samples.
896
897

Biogeosciences Discuss., doi:10.5194/bg-2016-222, 2016
Manuscript under review for journal Biogeosciences
Published: 3 June 2016

Table 2. Oxygen penetration depth (OPD), diffusive oxygen utilization (DOU) rate and O_2 consumption rate by aerobic respiration and re-oxidation of reduced inorganic compounds (RIC) in the pore water.

Station	OPD (mm)	DOU (mmol O_2 m^{-2} d^{-1})	O_2 consumption (mmol O_2 m^{-2} d^{-1}) by	
			Aerobic respiration	Re-oxidation of RIC
M1	3.2 (± 0.20)	7.12 (± 1.36)	4.04 (± 2.03)	3.07 (± 0.68)
D3	3.6 (± 0.03)	5.95 (± 0.16)	2.53 (± 0.72)	3.42 (± 0.58)

Values represent averages ± 1SD (n = 3)

Biogeosciences Discuss., doi:10.5194/bg-2016-222, 2016
Manuscript under review for journal Biogeosciences
Published: 3 June 2016

906 Table 3. Depth integrated rates (mmol m^{-2} d^{-1}) of Mn reduction, Fe reduction, and sulfate reduction and the partitioning of abiotic and
907 microbial Fe(III) reduction in total Fe(III) reduction with depth.

St.	Depth Interval (cm)	SO_4^{2-} Red	Mn Red	[a]Total Fe(III) Red	Fe reduction by		Fe $Red_{(Microbial)}$ / Fe $Red_{(Abiotic)}$
					[a]Abiotic Fe Red	[a]Microbial Fe Red	
M1	0 – 2	1.35	0.04	4.75	0.90	3.86	4.28
	2 – 4	1.04	-	3.02	0.70	2.33	3.33
	4 – 6	0.84	-	1.58	0.56	1.21	2.16
	6 – 8	0.54	-	1.25	0.36	0.89	2.47
	8 – 10	0.53	-	0.77	0.36	0.41	1.14
	Sum (0-10)	4.30	0.04	11.4	2.88	8.70	
D3	0 – 2	0.06	[b]3.19	-	-	-	n.a.
	2 – 4	0.11	3.96	1.63	0.07	1.56	22.3
	4 – 6	0.13	1.05	4.80	0.09	4.71	52.3
	6 – 8	0.06	0.01	0.86	0.04	0.83	20.8
	8 – 10	0.07	0.00	0.24	0.05	0.19	3.80
	Sum (0-10)	0.43	8.21	7.53	0.25	7.29	

908 [a]Stoichiometric equations were used to evaluate the relative significance of abiotic and microbial Fe reduction:
909 Abiotic reduction of Fe(III) by sulfide oxidation, $3H_2S + 2FeOOH = 2FeS + S^o + 4H_2O$; Microbial Fe(III) reduction = Total Fe(III) reduction – abiotic Fe(III) reduction.
910 [b]back-calculated from the C oxidation by Mn reduction in the 0 – 2 cm interval in Table 5 using the stoichiometric equation, $2MnO_2 + CH_2O + H_2O = 2Mn^{2+} + HCO_3^- + 3OH^-$.
911 ' – ' indicates that the process does not occur or is regarded as negligible at the depth interval based on the OPD for aerobic respiration and geochemical profiles or anoxic
912 bag incubations for Mn(IV) and Fe(III) reduction
913 'n.a.' indicates that data are not available.
914
915
916

Biogeosciences Discuss., doi:10.5194/bg-2016-222, 2016
Manuscript under review for journal Biogeosciences
Published: 3 June 2016

Table 4. Organic carbon (C_{org}) oxidation (mmol C m^{-2} d^{-1}) by each C_{org} oxidation pathway, and its partitioning in total C_{org} oxidation (% Total C_{ox}) and anaerobic C_{org} oxidation (% Anaerobic C_{org} ox) at each depth interval within 10 cm of the sediment. Mn Red, Mn reduction; Fe Red, Fe reduction; and SO_4^{2-} Red, sulfate reduction

St.	Depth Interval (cm)	C_{org} oxidation measured by		[c]Total C_{org} oxidation (DOU + DIC)	Anaerobic C_{org} oxidation by dissimilatory			Total anaerobic C_{org} oxidation (Mn Red + Fe Red + SO_4^{2-} Red)	Total Anaerobic C_{org} oxidation / Anoxic DIC production
		[a]DOU (Aerobic respiration)	[b]DIC prod. (Anaerobic respiration)		[d]Mn Red	[d,e]Fe Red	[d]SO_4^{2-} Red		
M1	0 – 2	3.11	5.59	8.70	0.02	0.96	2.69	3.67	0.66
	2 – 4	-	3.31	3.31	-	0.58	2.09	2.67	0.81
	4 – 6	-	2.26	2.26	-	0.26	1.67	1.93	0.85
	6 – 8	-	1.50	1.50	-	0.22	1.08	1.30	0.87
	8 – 10	-	1.37	1.37	-	0.10	1.06	1.17	0.85
	Sum (0 – 10)	3.11	14.0	17.1	0.02	2.13	8.59	10.7	0.77
	(% Total C_{org} ox)	(18.1)	(81.9)	(100)	(0.13)	(12.4)	(50.1)	(62.7)	
	(% Anaerobic C_{org} ox)				(0.16)	(15.2)	(61.2)		
D3	0 – 2	1.94	1.72	3.66	[f]1.59	-	0.13	1.72	1.00
	2 – 4	-	2.72	2.72	1.98	0.39	0.22	2.58	0.95
	4 – 6	-	2.32	2.32	0.52	1.18	0.26	1.96	0.84
	6 – 8	-	*0.30*	0.30	0.01	0.21	0.12	0.33	1.10
	8 – 10	-	*0.16*	0.16	-	0.05	0.15	0.19	1.21
	Sum (0 – 10)	1.94	*7.22*	9.2	4.10	1.82	0.86	6.79	0.94
	(% Total C_{org} ox)	(20.6)	(78.8)	(100)	(44.8)	(19.9)	(9.41)	(77.8)	
	(% Anaerobic C_{org} ox)				(56.8)	(25.2)	(11.9)		

[a] Aerobic C_{org} oxidation rate (= O_2 consumption by aerobic respiration x (106C/138O_2) calculated using the Redfield ratio; O_2 consumption by aerobic respiration rate (= DOU - re-oxidation rates) is calculated from Table 2 that is derived from the O_2 micro-profiles in Fig. 2.
[b] independently measured from the DIC accumulation rate in anoxic bag incubation experiment in Fig. 6 and 7.
[c] Total C_{org} oxidation = aerobic C_{org} oxidation + anaerobic C_{org}.oxidation
[d] C_{org} oxidation by dissimilatory Mn(IV) reduction, Fe(III) reduction, and sulfate reduction was calculated from the stoichiometric equations: $2MnO_2 + CH_2O + H_2O = 2Mn^{2+} + HCO_3^- + 3OH^-$; $4Fe(OH)_3 + CH_2O = 4Fe^{2+} + HCO_3^- + 7OH^-$; $SO_4^{2-} + 2CH_2O = H_2S + 2HCO_3^-$, $H_2S = HS^- + H^+$
[e] Dissimilatory Fe(III) reduction = (Total Fe(III) reduction in Fig.7) – (Abiotic Fe(III) reduction coupled to H_2S oxidation; $3H_2S + 2FeOOH = 2FeS + S^o + 4H_2O$)
[f] back-calculated from: DIC production rate - (C oxidation by SO_4^{2-} Red and Fe Red). See text for further discussion
' – ' indicates that the process does not occur or is regarded as negligible based on the OPD for aerobic respiration and geochemical profiles or anoxic bag incubations for Mn and Fe Red.

Biogeosciences Discuss., doi:10.5194/bg-2016-222, 2016
Manuscript under review for journal Biogeosciences
Published: 3 June 2016

Figure legends

Fig. 1. Sampling stations in the East Sea and pictures showing contrasting colors between surface sediments of the continental slope (M1) and center of the basin (D3)

Fig. 2. Concentrations of dissolved NH_4^+, NO_3^-, Mn^{2+} and Fe^{2+} in pore water and solid phase $Mn_{(DCA)}$, $Fe(II)_{(oxal)}$, $Fe(III)_{(oxal)}$, acid volatile sulfur (AVS) and chromium reducible sulfur (CRS) in the sediment at M1 and D3.

Fig. 3. Vertical profiles of O_2. The slashed area indicates the diffusive boundary layer in the sediment-water interface. The shaded area indicates that O_2 consumption by aerobic respiration (I and II) and re-oxidation of reduced inorganic compounds (III), respectively.

Fig. 4. Changes in pore water concentrations of DIC, Ca^{2+} and Mn^{2+} and solid phase $Fe(II)_{(oxal)}$ during anoxic bag incubations of sediments from 0-2, 2-4, 4-6, and 6-8 cm depth at M1 and D3. Data obtained at 8-10 cm depth interval is not shown.

Fig. 5. Vertical distribution of terminal electron acceptors (O_2, NO_3^-, Mn and Fe) and rates of sulfate reduction measured from whole core analyses, and rates of anaerobic carbon oxidation (DIC production rates), Mn reduction and Fe reduction measured from anoxic bag incubations in Fig. 4. C_{org} by sulfate reduction in panel C and H was calculated from the stoichiometry of 2:1 of C_{org} oxidized to sulfate reduced.

Fig. 6. Depth variations of partitioning of each carbon oxidation pathway in total carbon oxidation at M1 and D3

Fig. 7. The relative contribution of Mn reduction to total carbon oxidation as a function of the concentration of Mn(DCA) at 3 different sites. BS, Black Sea (Thamdrup et al. 2000); UB, Ulleung Basin (This study); Sk, Skagerrak (Canfield et al. 1993b).

Biogeosciences Discuss., doi:10.5194/bg-2016-222, 2016
Manuscript under review for journal Biogeosciences
Published: 3 June 2016

Hyun et al. – Figure 1

Fig. 1. Sampling stations in the East Sea and pictures showing contrasting colors between surface sediments of the continental slope (M1) and center of the basin (D3)

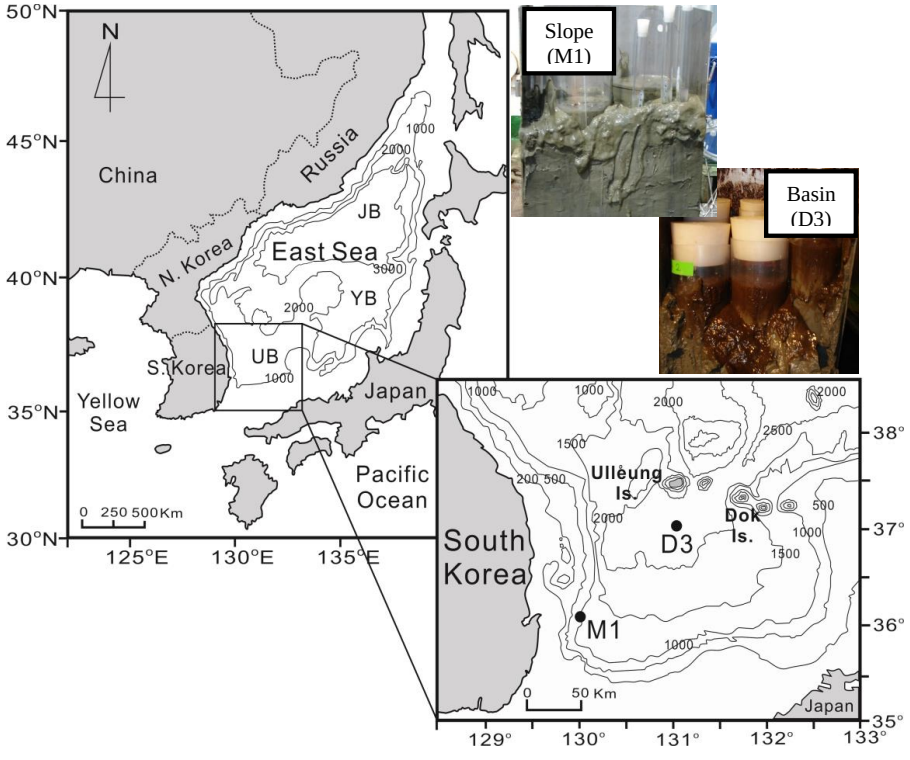

Biogeosciences Discuss., doi:10.5194/bg-2016-222, 2016
Manuscript under review for journal Biogeosciences
Published: 3 June 2016

Biogeosciences
Discussions
Open Access
EGU

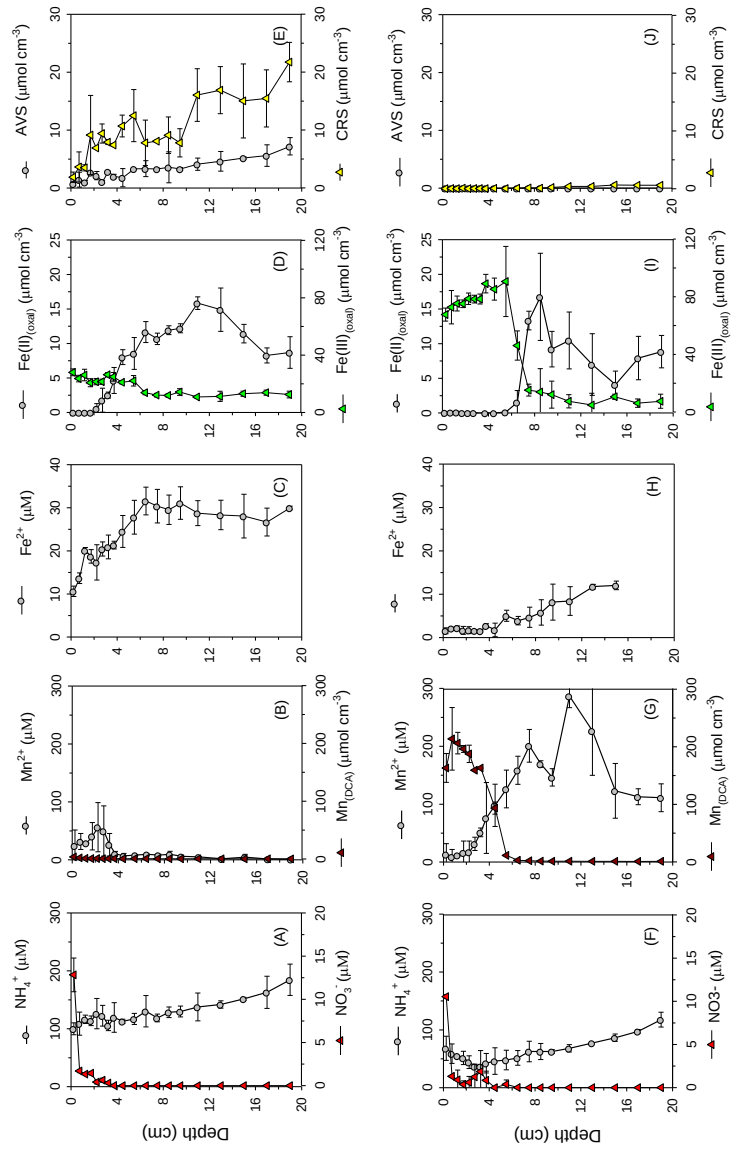

Hyun et al – Figure 2

Fig. 2. Concentrations of dissolved NH_4^+, NO_3^-, Mn^{2+} and Fe^{2+} in pore water and solid phase $Mn_{(DCA)}$, $Fe(II)_{(oxal)}$, $Fe(III)_{(oxal)}$, acid volatile sulfur (AVS) and chromium reducible sulfur (CRS) in the sediment at M1 and D3

Biogeosciences Discuss., doi:10.5194/bg-2016-222, 2016
Manuscript under review for journal Biogeosciences
Published: 3 June 2016

Hyun et al – Figure 3

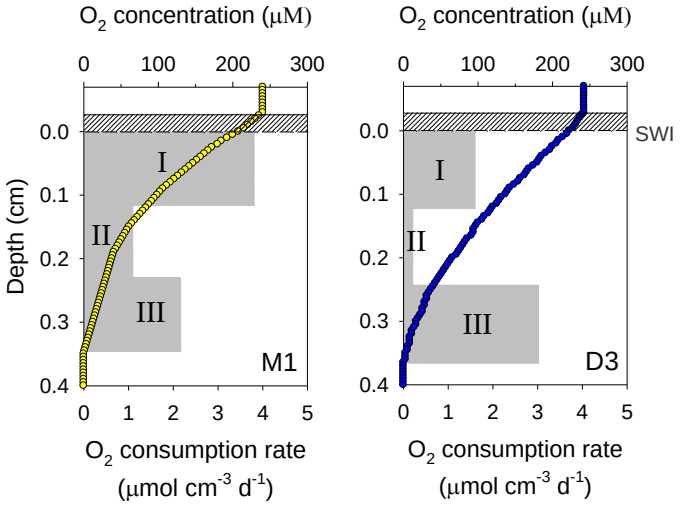

Fig. 3. Vertical profiles of O_2 The slashed area indicates diffusive boundary layer in the sediment-water interface. The shaded area indicates that O_2 consumption by aerobic respiration (I and II) and re-oxidation of reduced inorganic compounds (III), respectively.

Biogeosciences Discuss., doi:10.5194/bg-2016-222, 2016
Manuscript under review for journal Biogeosciences
Published: 3 June 2016

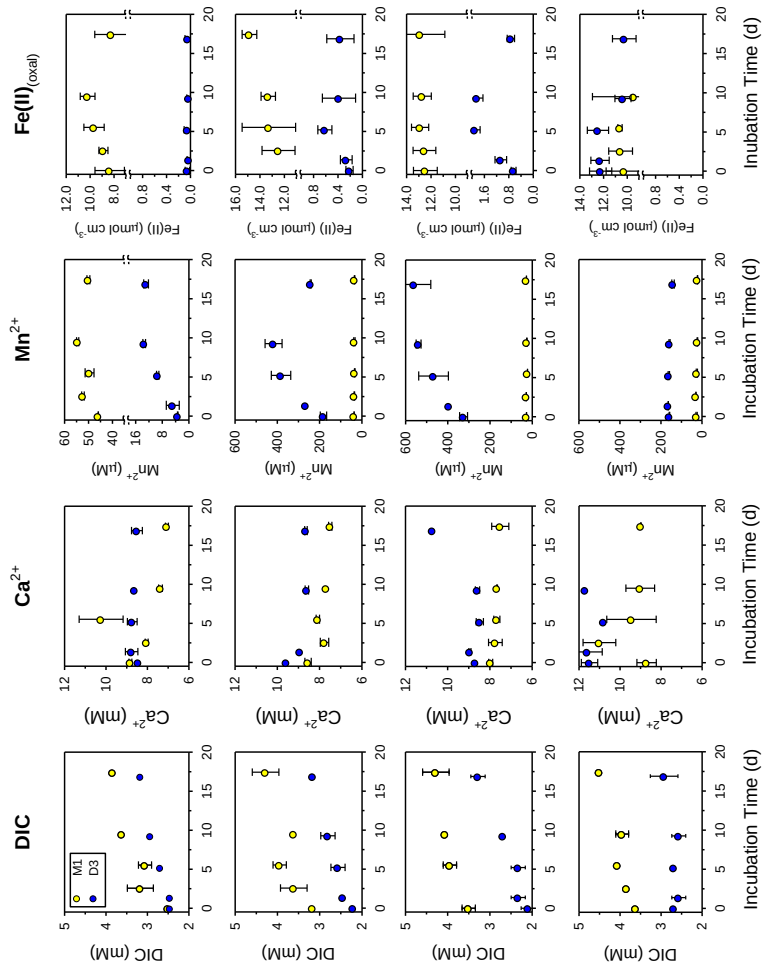

Hyun et al – Figure 4

Fig. 4. Changes in pore water concentrations of DIC, Ca^{2+} and Mn^{2+} and solid phase $Fe(II)_{(oxal)}$ during anoxic bag incubations of sediments from 0-2, 2-4, 4-6, and 6-8 cm depth at M1 and D3. Data obtained at 8-10 cm depth interval is not shown.

Biogeosciences Discuss., doi:10.5194/bg-2016-222, 2016
Manuscript under review for journal Biogeosciences
Published: 3 June 2016

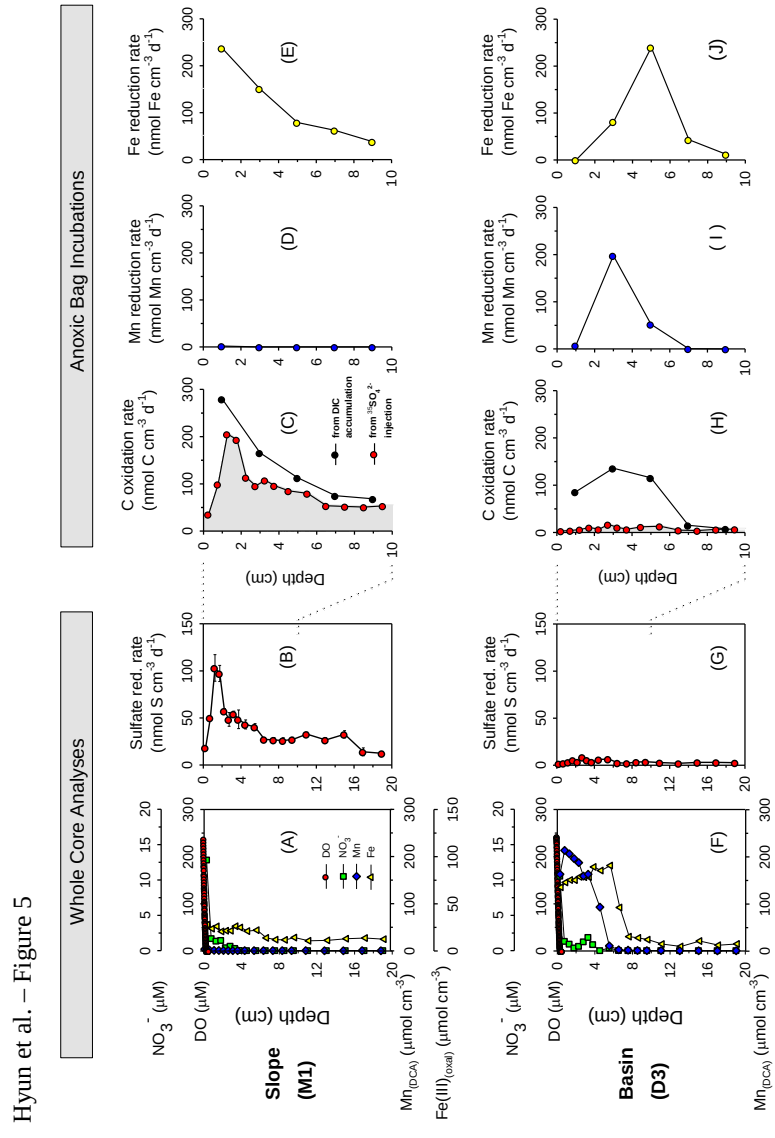

Hyun et al. – Figure 5

Fig. 5. Vertical distribution of terminal electron acceptors (O_2, NO_3^-, Mn and Fe) and rates of sulfate reduction measured from whole core analyses, and rates of anaerobic carbon oxidation (DIC production rates), Mn reduction and Fe reduction measured from anoxic bag incubations in Fig. 4. C_{org} by sulfate reduction in panel C and H was calculated from the stoichiometry of 2:1 of C_{org} oxidized to sulfate reduced.

Biogeosciences Discuss., doi:10.5194/bg-2016-222, 2016
Manuscript under review for journal Biogeosciences
Published: 3 June 2016

Hyun et al. – Figure 6

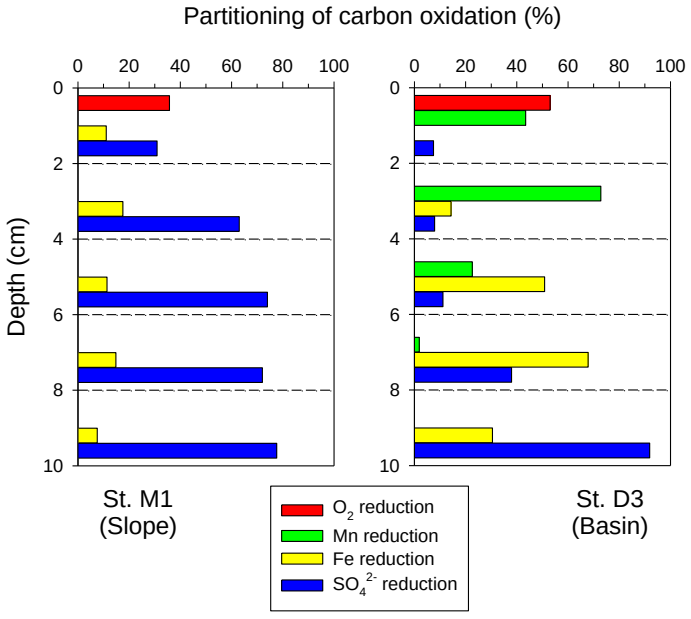

Fig. 6. Depth variations of partitioning of each carbon oxidation pathway in total carbon oxidation at M1 and D3

Biogeosciences Discuss., doi:10.5194/bg-2016-222, 2016
Manuscript under review for journal Biogeosciences
Published: 3 June 2016

Hyun et al - Figure 7

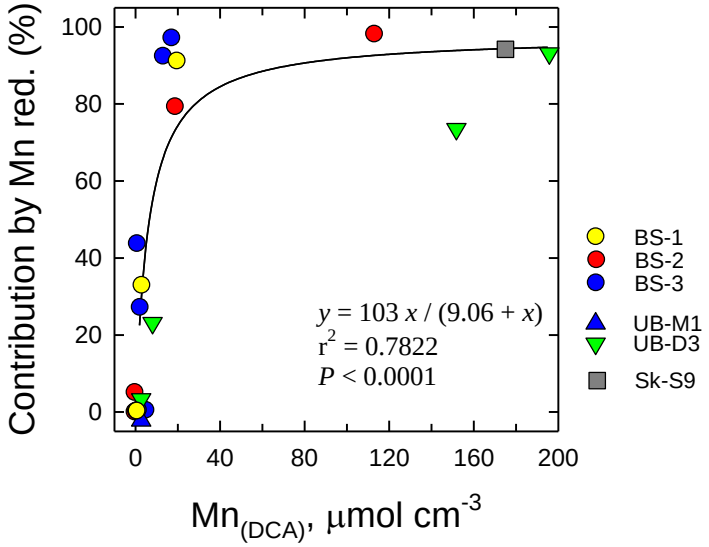

Fig. 7. The relative contribution of Mn reduction to total carbon oxidation as a function of the concentration of Mn(DCA) at 3 different sites. BS, Black Sea (Thamdrup et al. 2000); UB, Ulleung Basin (This study); Sk, Skagerrak (Canfield et al. 1993b).